

# Supporting Information

## Table of contents

Experimental Section.....	2
<b>Generation of stably transfected HEK293 cell lines containing the opsin genes</b> .....	2
<b>Expression and purification of selectively <sup>15</sup>N tryptophan, labeled rhodopsin from HEK293S cells</b> .....	2
<b>Expression and purification of Tr</b> .....	3
<b>Real-time NMR spectroscopy</b> .....	3
Tr-rhodopsin interaction.....	3
<b>Flash photolysis</b> .....	4
Tr-rhodopsin interaction.....	4
<b>Global Lifetime Analysis (GLA) and Lifetime Density Analysis (LDA)</b> .....	5
References .....	7
Supplementary figures.....	8
<b>Figure S1:</b> Schematic diagram for the laser setup of NMR and flash photolysis experiment. ....	8
<b>Figure S2:</b> NMR kinetic data. ....	9
<b>Figure S3:</b> Global lifetime analysis.....	10
<b>Table S1:</b> The lifetimes, the distribution maxima and the amplitudes of the signatures C-F of the LDMs of rhodopsin.....	11

## **Experimental Section**

### **Generation of stably transfected HEK293 cell lines containing the opsin genes**

Previously in our group the wild type opsin gene was cloned to pACMV-tetO vector to enable expression in stably transfected HEK293 cells.<sup>[1,2]</sup> The pACMV-tetO vector was originally developed by Reeves et al.<sup>[3,4]</sup> The preparation of stably transfected HEK293 cell lines containing the opsin gene was carried out as described previously.<sup>[4,5]</sup>

### **Expression and purification of selectively <sup>15</sup>N tryptophan, labeled rhodopsin from HEK293S cells**

Rhodopsin was expressed in tetracycline inducible HEK293 cells. For the expression of the wild type opsin gene, the cells were grown in 143 cm<sup>2</sup> cell culture petri dishes. The cells were induced using cell culture media consisting of individual components enabling a selective isotope labeling scheme.<sup>[4,6]</sup> Cells were harvested 2 - 3 days after induction. For sample preparation, cells harvested from 150 - 200 (for NMR experiments) or 50 - 70 (for flash photolysis experiments) petri dishes were resuspended in phosphate buffered saline (PBS) at pH 7.4. 11-cis-retinal was added to the cell suspension at a final concentration of 40 μM. 11-cis-retinal was prepared by illuminating all-trans-retinal and subsequent separation of the obtained isomers as previously described.<sup>[7]</sup> Rhodopsin was solubilized by addition of 1% DDM (n-Dodecyl-β-D-maltoside) and purified via immunoaffinity chromatography. The 1D4 antibody (obtained from University of British Columbia, Vancouver, Canada) was coupled to activated Sepharose 4B as previously described.<sup>[8]</sup> Rhodopsin was bound to the beads and washed with 10 column volumes of buffer A (25 mM Tris buffer at pH 7.5 + 0.05 % DDM). The detergent exchange was performed on the column by applying 10 column volumes of buffer B (buffer A + 0.2 % DHPC (1,2-diheptanoyl-*sn*-

glycero-3-phosphocholine)). Rhodopsin was subsequently eluted with buffer B containing the peptide TETSQVAPA at a concentration of 100  $\mu\text{M}$ . Fractions containing rhodopsin were pooled and concentrated by amicon centrifuge concentrator (Millipore, Billerica, USA).

### **Expression and purification of Tr**

The procedure for expression and purification of Tr was published previously.<sup>[9]</sup>

### **Real-time NMR spectroscopy**

**Tr-rhodopsin interaction.** NMR experiments of bovine rhodopsin were performed with a protein concentration of 150  $\mu\text{M}$  in 25 mM Tris buffer at pH 7.5. Rhodopsin was solubilized in the detergent DHPC (1.5 - 2 % (w/v)). For interaction studies, rhodopsins in DHPC micelles were mixed with two fold higher concentration of Tr (300  $\mu\text{M}$ ) in the same buffer.

$^1\text{H}$ ,  $^{15}\text{N}$  SOFAST-HMQC<sup>[10,11]</sup> (Heteronuclear Multiple Quantum Correlation) experiments were performed to determine chemical shift perturbations in tryptophan residues of rhodopsin to map the structural differences in rhodopsin upon solubilization in DDM and DHPC micelles.  $^1\text{H}$ ,  $^{15}\text{N}$  SOFAST-HMQC spectra were also recorded to structurally map the interaction between Tr and rhodopsin in the dark state.

Real-time NMR experiments were conducted on a Bruker Avance I 800 MHz spectrometer at  $T = 298\text{ K}$ . An argon ion laser with emission wavelength  $\lambda = 514\text{ nm}$  was used for the illumination of the rhodopsin sample. The laser beam was directly guided into the NMR sample via an optical fiber (Figure S1 a).<sup>[12]</sup> A cw-beam of 300 mW was applied for 0.5 s to trigger the photocycle of rhodopsin.

Photodynamics of rhodopsin in absence or presence of Tr were studied by recording a series of one dimensional  $^1\text{H}$  X-filtered<sup>[13]</sup> spectra in a pseudo two dimensional manner. X-filter experiments were performed to avoid resonance ambiguities and simplify the NMR spectrum. The temporal resolution of the one dimensional experiments was  $\sim 1$  minute. The focus was on the indole region of the spectrum where the indole side chain signals of the tryptophan residues are to be expected (with a carrier frequency of 10.6 kHz and a spectral width of 833.3 Hz).

Rhodopsin kinetics was extracted from these 1D  $^1\text{H}$  X-filtered spectra. The kinetic behavior of individual amino acids was determined by applying an exponential decay fitting model on the corresponding signal row as follows:

$$I(t) = a + b * e^{-t/\tau}$$

Variable  $a$  is the offset,  $b$  is the amplitude and variable  $\tau$  is the lifetime.

## Flash photolysis

**Tr-rhodopsin interaction.** Transient absorption measurements were performed with a home-built flash photolysis setup (Figure S1 b). The samples were photoexcited using a single ns-pulse with the central wavelength of  $\lambda_{\text{max}}=500$  nm using a Nd:YAG laser (Spitlight 600, Innolas Laser GmbH) and an optical parametric oscillator (OPO, preciScan, GWU-Lasertechnik). For probing the absorption change, the transmitted intensity from a xenon flash lamp that provides spectrally broad  $\mu\text{s}$ -pulses, was detected. The transmitted intensity  $I_{\text{sig}}(\lambda, t)$  was measured with an ICCD camera (PI-MAX 3, Princeton Instruments). To increase the signal-to-noise ratio the intensity spectrum of the detection light  $I_{\text{ref}}(\lambda, t)$  was measured separately. In the same manner, the transmission of the sample and the reference were measured before the

photoexcitation event,  $I_{sig}^0(\lambda)$  and  $I_{ref}^0(\lambda)$ . Based on this, the change in absorption was calculated as follows:

$$\Delta A(\lambda, t) = -\log\left(\frac{I_{sig} * I_{ref}^0}{I_{ref} * I_{sig}^0}\right)$$

Since the rhodopsin photodynamics is not cyclic, only a single non-repetitive measurement could be conducted. Hence, the measurements had a relatively low signal-to-noise ratio. The spectral range of detection is 316 – 649 nm and the spectral resolution was ~0.5 nm. The raw data set was binned into wavelength resulting in a resolution of ~10 nm. The analysis of the data was performed entirely based on the binned data. The temporal resolution of the measurements was 1 sec within a range from 0 to 10 min. The sample for these experiments consist of DHPC solubilized rhodopsin (25  $\mu$ M) in a 20 mM Tris buffer at pH 7.4 and Tr with increasing concentration from 0  $\mu$ M to 100  $\mu$ M. All the experiments were performed at room temperature.

### **Global Lifetime Analysis (GLA) and Lifetime Density Analysis (LDA)**

Typically, transient absorption data were analyzed by global lifetime analysis (GLA) using sums of a small number ( $\sim < 10$ ) of exponentials:

$$I(\lambda, t) = \sum_{i=1}^n A_i(\lambda) e^{-\frac{t}{\tau}}$$

with  $t$  for time,  $\tau$  for the lifetime, and  $\lambda$  for the wavelength.

In GLA, the number of exponential functions determines the complexity of the kinetic process. Thus, the data analysis is model-dependent that determines decay associated spectra  $A_i(\lambda)$  (DAS) for each fitted lifetime. In DAS, the positive pre-exponential amplitudes (red) describe either decay of absorption or the rise of

bleaching, while negative pre-exponential amplitudes (blue) reflect either decay of bleaching or the rise of absorption.

However, the spectral signature of the photodecay kinetics of rhodopsin consists of spectrally and temporally interfering signals. In addition, the decay cycle involving linear and branched intermediates may result in non-exponential processes. Both aspects make the interpretation of the resulting decay-associated spectra (DAS) ambiguous. Therefore, we additionally performed a lifetime density analysis (LDA). With this method the pre-exponential amplitudes  $\Phi(\lambda, \tau)$  of the sum of a large number (typically  $\sim 100$ ) of exponential functions were determined. For each exponential function, the lifetime was fixed. Time-resolved data are quantitatively modelled by a spectrum of lifetimes,  $\tau$ :

$$I(\lambda, t) = \int_0^{\infty} \Phi(\lambda, \tau) e^{-t/\tau} d\tau$$

where  $I(\lambda, t)$  is the normalized decay function and  $\Phi(\lambda, \tau)$  is the spectral density function. An inverse Laplace transform of  $I(\lambda, t)$  was performed to determine  $\Phi(\lambda, \tau)$ . Hence, LDA covers a spectrally resolved distribution for each lifetime. The results can be presented in the form of a contour map, which is designated as lifetime density map (LDM). The maps can be read in the similar manner as described for DAS. In contrast to GLA, LDA is model-independent. Moreover, it can also reveal non-exponential or stretched exponential kinetics which cannot be determined in GLA.

## References

- [1] J. Stehle, R. Silvers, K. Werner, D. Chatterjee, S. Gande, F. Scholz, A. Dutta, J. Wachtveitl, J. Klein-Seetharaman, H. Schwalbe, *Angew. Chem. Int. Ed. Engl.* **2014**, *53*, 2078–2084.
- [2] J. Stehle, R. Silvers, K. Werner, D. Chatterjee, S. Gande, F. Scholz, A. Dutta, J. Wachtveitl, J. Klein-Seetharaman, H. Schwalbe, *Angew. Chemie* **2014**, *126*, 2110–2116.
- [3] P. J. Reeves, J.-M. Kim, H. G. Khorana, *Proc. Natl. Acad. Sci. U. S. A.* **2002**, *99*, 13413–13418.
- [4] P. J. Reeves, N. Callewaert, R. Contreras, H. G. Khorana, *Proc. Natl. Acad. Sci. U. S. A.* **2002**, *99*, 13419–13424.
- [5] M. C. Loewen, J. Klein-Seetharaman, E. V Getmanova, P. J. Reeves, H. Schwalbe, H. G. Khorana, *Proc. Natl. Acad. Sci. U. S. A.* **2001**, *98*, 4888–4892.
- [6] K. Werner, C. Richter, J. Klein-Seetharaman, H. Schwalbe, *J. Biomol. NMR* **2008**, *40*, 49–53.
- [7] A. Knowles, A. Priestley, *Vision Res.* **1978**, *18*, 115–116.
- [8] D. D. Oprian, R. S. Molday, R. J. Kaufman, H. G. Khorana, *Proc. Natl. Acad. Sci. U. S. A.* **1987**, *84*, 8874–8878.
- [9] V. V. Gurevich, *J. Biol. Chem.* **1998**, *273*, 15501–15506.
- [10] P. Schanda, E. Kupce, B. Brutscher, *J. Biomol. NMR* **2005**, *33*, 199–211.
- [11] P. Schanda, B. Brutscher, *J. Am. Chem. Soc.* **2005**, *127*, 8014–8015.
- [12] T. Kühn, H. Schwalbe, *J. Am. Chem. Soc.* **2000**, *122*, 6169–6174.
- [13] E. Woergoetter, G. Wagner, K. Wuethrich, *J. Am. Chem. Soc.* **1986**, *108*, 6162–6167.
- [14] A. Bax, D. G. Davis, *J. Magn. Reson.* **1985**, *65*, 355–360.
- [15] M. Piotto, V. Saudek, V. Sklenář, *J. Biomol. NMR* **1992**, *2*, 661–665.
- [16] V. Sklenar, M. Piotto, R. Leppik, V. Saudek, *J. Magn. Reson. Ser. A* **1993**, *102*, 241–245.
- [17] T. L. Hwang, A. J. Shaka, *J. Magn. Reson. Ser. A* **1995**, *112*, 275–279.
- [18] J. Granzin, U. Wilden, H. W. Choe, J. Labahn, B. Krafft, G. Büldt, *Nature* **1998**, *391*, 918–921.

## Supplementary figures

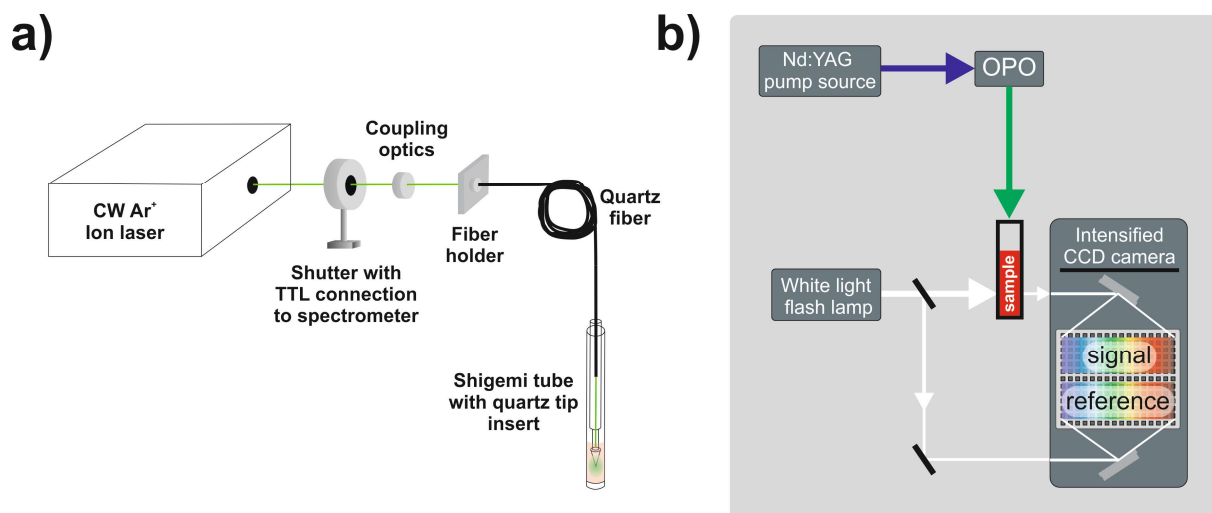


**Figure S1:** Schematic diagram for the laser setup of NMR and flash photolysis experiment. a) NMR. The laser beam emitted at  $\lambda = 514$  nm and guided directly into a quartz fiber by coupling optics. The end of the quartz fiber was attached to a shigemi tube with the sample. b) Flash photolysis. The pump pulse was generated by an optical parametric oscillator (preciScan, GWU-Lasertechnik) and an Nd:YAG laser system (Spitlight 600, Innolas Laser GmbH). The excitation wavelength was adjusted to 500 nm (absorption maximum of dark-state bovine rhodopsin). For detection a xenon white light flash lamp was used. The transmission of these pulses (indicated as *signal* in the scheme) was measured via an ICCD detector (PI-MAX3, Princeton Instruments). Simultaneously the spectrum of the detection light was measured (indicated as *reference* in the scheme) in order to increase the signal-to-noise ratio.



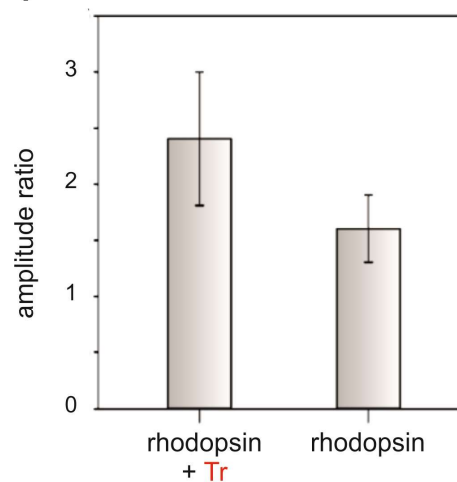
a)

rhodopsin	lifetime (min)	amplitude ratio ( $\xi$ )
W35 (meta III)	$6.9 \pm 0.4$	$1.6 \pm 0.3$
W126 (meta II)	$5.0 \pm 0.4$	

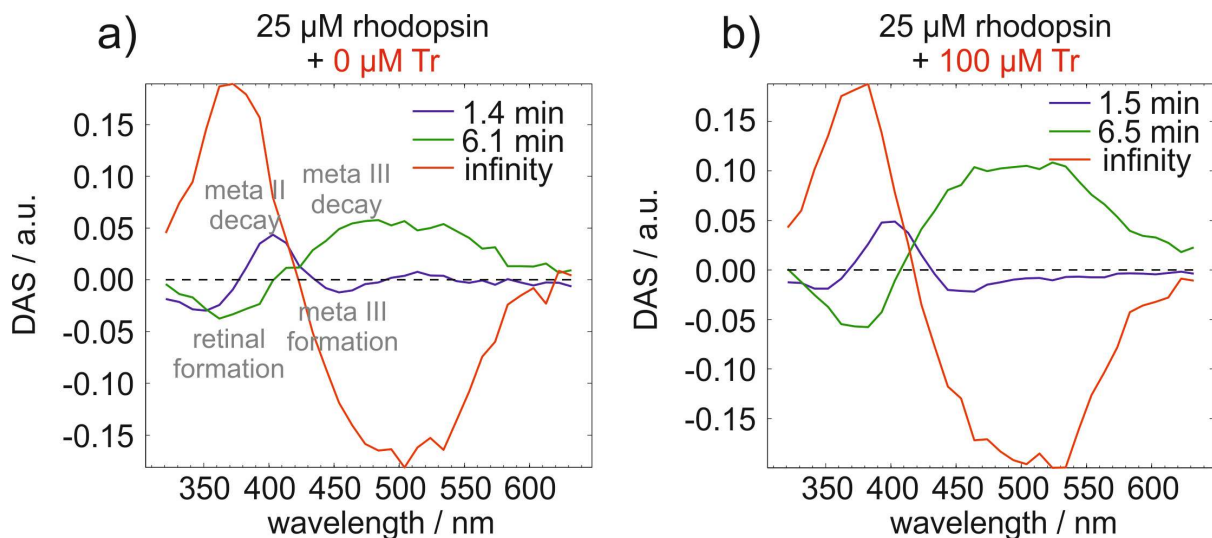
  

rhodopsin + Tr	lifetime (min)	amplitude ratio ( $\xi$ )
W35 (meta III)	$9.6 \pm 1.9$	$2.4 \pm 0.6$
W126 (meta II)	$5.2 \pm 2.1$	

b)



**Figure S2:** NMR kinetic data. a) Lifetime and initial amplitude ratio of W35 and W126 indole resonances (above – rhodopsin, below – rhodopsin + Tr) as extracted from the exponential fit (Figure 3b). b) Graphical representation of the amplitude ratios of W35 and W126 with error bars.



**Figure S3:** Global lifetime analysis. Decay associated spectra (DAS) from the global lifetime analysis (GLA) of the transient absorption data in the absence (a) and presence (b) of Tr. The GLA provides **one fast lifetime (blue curve; 1-2 min)** corresponding to meta II decay (~400 nm), the free retinal release (~350 nm) and the formation of meta III (~460 nm), **one slower lifetime (green curve; 6-7 min)** corresponding to the decay of meta III (above 450 nm) and the formation of free retinal (370 nm) and **one infinity lifetime (red curve)** corresponding to the change in absorption at the end of the photodynamics. In the presence of Tr the DAS signatures for the formation and decay of meta III (~460 nm) were more pronounced.

**Table S1:** The lifetimes, the distribution maxima and the amplitudes of the signatures C-F of the LDMs of rhodopsin (25  $\mu\text{M}$ ) in absence (-) and presence (10  $\mu\text{M}$  / 50  $\mu\text{M}$  / 100  $\mu\text{M}$ ) of Tr.

	lifetime / min				wavelength / nm				amplitude / a.u.			
	0 $\mu\text{M}$ Tr	10 $\mu\text{M}$ Tr	50 $\mu\text{M}$ Tr	100 $\mu\text{M}$ Tr	0 $\mu\text{M}$ Tr	10 $\mu\text{M}$ Tr	50 $\mu\text{M}$ Tr	100 $\mu\text{M}$ Tr	0 $\mu\text{M}$ Tr	10 $\mu\text{M}$ Tr	50 $\mu\text{M}$ Tr	100 $\mu\text{M}$ Tr
C <sup>[1]</sup>	1.3	1.6	1.5	1.5	400	400	400	390	0.003	0.003	0.004	0.004
D <sup>[2]</sup>	1.2	1.0	1.1	1.3	465	465	465	465	-0.001	-0.002	-0.003	-0.004
E <sup>[3]</sup>	5.0	5.0	5.5	5.3	460-540	460-540	460-540	460-540	0.003	0.006	0.007	0.007
F <sup>[4]</sup>	2.5	2.7	2.7	5.3	365	355	365	375	-0.004	-0.003	-0.004	-0.004

[1] meta II decay [2] meta III formation [3] meta III decay [4] free retinal formation